Residual erythropoiesis protects against myocardial hemosiderosis in transfusion-dependent thalassemia by lowering labile plasma iron via transient generation of apotransferrin

by Maciej W. Garbowski, Patricia Evans, Evangelia Vlachodimitropoulou, Robert Hider and John B. Porter

Haematologica 2017 [Epub ahead of print]

Citation: Garbowski MW, Evans P, Vlachodimitropoulou E, Hider R and Porter JB. Residual erythropoiesis protects against myocardial hemosiderosis in transfusion-dependent thalassemia by lowering labile plasma iron via transient generation of apotransferrin. Haematologica. 2017; 102:xxx doi:10.3324/haematol.2017.170605

Title Page

Title:
Residual erythropoiesis protects against myocardial hemosiderosis in transfusion-dependent thalassemia by lowering labile plasma iron via transient generation of apotransferrin.

Names of authors: Maciej W. Garbowski[1,2], Patricia Evans[1], Evangelia Vlachodimitropoulou[1], Robert Hider[3], and John B. Porter[1,2]

Authors' affiliations:
[1]Research Haematology Department, Cancer Institute, University College London, UK
[2]University College London Hospitals, London, UK
[3]Institute of Pharmaceutical Sciences, King's College London, UK

Running heads:
Thalassemic erythropoiesis, LPI, and cardiac iron.

Contact information for correspondence: Dr Maciej Garbowski, Research Haematology Department, UCL Cancer Institute, Paul O'Gorman Building, 72 Huntley Street, WC1E 6BT, London, UK, maciej.garbowski@ucl.ac.uk, phone: +44 207 679 6233, fax +44 207 679 6224

Word count
Abstract 249
Main text 3994
Number of tables 1
Number of Figures 5
Number of references 50
Online supplement 1

Acknowledgements
The authors would like to thank Dr. Sukhvinder Bansal from the Department of Pharmacy at King's College London for performing the hepcidin assay. MG would like to thank Dr. Farrukh Shah for co-supervision of Ph.D.; British Society for Haematology, Sickle Cell Society and UK Thalassaemia Society for the Haemoglobinopathy Fellowship Grant, as well as Leukaemia and Blood Diseases Appeal for grant support. JP would like to thank UCL Biomedical Research Centre for Cardiometabolic Programme support. All authors also would like to thank Wellcome Trust for grant support (WT093209MA).

Abstract

Cardiosiderosis is a leading cause of mortality in transfusion-dependent thalassemias. Plasma non-transferrin-bound iron and its redox-active component, labile plasma iron, are key sources of iron loading in cardiosiderosis. Risk factors were identified in 73 patients with or without cardiosiderosis. Soluble transferrin receptor-1 levels were significantly lower in patients with cardiosiderosis (odds ratio 21). This risk increased when transfusion-iron loading rates exceeded the erythroid transferrin uptake rate (derived from soluble transferrin receptor-1) by >0.21mg/kg/d (odds ratio 48). Labile plasma iron was >3-fold higher where this uptake rate threshold was exceeded, but non-transferrin-bound iron and transferrin saturation were comparable. Cardiosiderosis risk was also decreased in patients with low liver iron, ferritin and labile plasma iron, or high bilirubin, reticulocyte counts or hepcidin. We hypothesized that high erythroid transferrin uptake rate decreases cardiosiderosis through increased erythroid re-generation of apotransferrin. To test this, iron uptake and intracellular reactive oxygen species were examined in HL-1 cardiomyocytes under conditions modelling transferrin effects on non-transferrin-bound iron speciation with ferric citrate. Intracellular iron and reactive oxygen species increased with ferric citrate concentrations especially where iron-to-citrate ratios exceeded 1:100, i.e. conditions favoring kinetically labile monoferric rather than oligomer species. Excess iron-binding equivalents of apotransferrin inhibited iron uptake, decreased intracellular reactive oxygen species and labile plasma iron, under conditions favoring monoferric species. In conclusion, high transferrin iron utilisation, relative to the transfusion-iron load rate, decreases the cardiosiderotic risk. A putative mechanism is the transient re-generation of apotransferrin by an active erythron, rapidly binding labile plasma iron-detectable ferric monocitrate species.

Introduction

Cardiosiderosis or myocardial hemosiderosis (MH) is a leading cause of mortality in transfusion-dependent thalassemias[1]. Suggested risk factors for MH and/or consequent cardiomyopathy have included: sustained high serum ferritin levels[2], high liver iron concentrations (LIC)[3], poor chelation adherence[4], as well as genetic susceptibility factors[5]. However, while improved monitoring by cardiac MRI and improved use of iron chelators[6] have led to falling frequencies of MH judged by cardiac MRI, there remains a variable prevalence between populations[7] and between individuals that is not fully understood.

The conduit through which MH develops is plasma non-transferrin-bound iron (NTBI), as transferrin-mediated iron uptake by cardiomyocytes is relatively 'insignificant'[8]. NTBI is detectable as chelatable iron[9,10] or redox-active iron (labile plasma iron, LPI)[11] at transferrin saturations >75% for NTBI[12] or 100% in the case of LPI[13]. Animal data suggest that NTBI is taken into myocardium through the L-type calcium channels[14], supported by recent clinical data where MH was inhibited in transfusion-dependent thalassemia patients by the calcium channel blocker amlodipine[15]. Plasma NTBI is not a single entity, however, being a heterogeneous multispeciated pool of ferric iron (not bound to high-affinity transferrin iron-binding sites) containing monomeric, oligomeric, and polymeric iron citrate species[16] with weak albumin binding[17], or stronger binding, where post-translational modifications to albumin occur[18]. There are a number of potential non-protein ligands for NTBI, including phosphate, acetate, amino acids, pyrophosphate, and citrate. However, phosphate, acetate, and amino acids cannot compete with the hydroxyl ion for iron(III) at pH 7.4. Pyrophosphate is potentially a potent iron(III) ligand but has a vanishingly small concentration in plasma after accounting for the effect of magnesium and calcium binding, thus citrate is the dominant ligand. The iron-to-citrate ratio determines the mix of species present. As plasma citrate is roughly constant at 100µM, the iron-to-citrate ratio is determined by the plasma NTBI concentrations. At 1µM NTBI the citrate excess is 100-fold and chelatable iron citrate species predominate, whereas, at ≥10µM NTBI, the proportion of chelatable iron drops substantially[17,19]. LPI refers to the redox-active fraction of NTBI, hence its term ‘labile’, which is chelatable[20], and has been implicated in organ hemosiderosis[21]. Its chemical nature is not characterized, although it is predicted to comprise both monomeric and oligomeric ferric citrate, albumin iron complexes, and possibly partially coordinated iron chelates, e.g. of deferiprone[22], that are able to form hydroxyl radicals in presence of ascorbate and hydrogen peroxide.

The balance between the rate of transferrin iron utilisation by the erythron and transfusion iron loading rate is key to determining levels of plasma NTBI[23]. Blood transfusion delivers a mean of 0.4mg/kg/day but with a wide range (0.2-0.6mg/kg/day)[24], exceeding by 10-fold the gut iron loading rate seen in non-transfusion-dependent thalassemia[25]. Transfused red cells are ultimately catabolised within macrophages of spleen, liver, and bone marrow, with iron released onto transferrin and -- when the latter approaches saturation -- forming plasma NTBI. Transferrin iron uptake by the erythron via transferrin receptor-1 (TfR1) liberates iron from transferrin during receptor-mediated endocytosis, whereupon iron-free apotransferrin is recycled back to plasma, for a detailed review, see *Gkouvatsos et al 2012*[26]. The extracellular domain of the transferrin receptor-1 is shed by red cell

progenitors and circulates bound to holotransferrin (sTfR1)[27]. TfR1 expression in the erythron is transcriptionally regulated such that levels increase in iron deficiency[28]. However, in thalassaemias, sTfR1 levels primarily reflect the degree of expansion of the erythron[29–31]. Blood transfusion suppresses expansion and activity of the erythron, thereby decreasing sTfR1 proportionately to the pre-transfusion hemoglobin[32].

In this paper, we have examined clinical factors associated with MH as well as the mechanisms underlying these associations. In particular, we have focussed on how transferrin-iron utilisation by the erythron marked by sTfR1, relative to the transfusion-iron loading rate, impacts on the risk of MH. We have considered how apotransferrin formed after endocytosis in the bone marrow may bind NTBI species, decreasing their availability for myocardial uptake.

Methods

Patients

A cohort of 73 transfusion-dependent thalassemia patients on deferasirox, with known transfusion-iron load rate[24], was divided into those with MH (n=24, cardiac T2*<20ms, R2*>50s^{-1}) and those without MH (n=49, T2*>20ms, R2* <50s^{-1})[33]. Details are provided in the **Supplement**. Patients gave written informed consent to participate in the study and approval was obtained from The Joint University College London/University College London Hospitals Committees on Ethics of Human Research.

Biomarkers

Pre-transfusion samples were tested, after a 48-hour washout from deferasirox chelation, for iron metabolism and routine biochemical variables, and compared in both groups (±MH). These included assays for NTBI[9], LPI[11], hepcidin, urea-gel transferrin saturation, sTfR1, GDF-15 as published previously[23], as well as routine clinical variables (hemoglobin, absolute reticulocyte count, nucleated red cells, serum ferritin, bilirubin, and serum iron), with further details in the **Supplement**.

Cell-line experiments

Murine HL-1 cardiomyocytes (ATCC number CRL-12197) were grown in Claycomb medium (Sigma); the culture protocol is described in the **Supplement**. Buffered ferric citrate[17,16] or ferric ammonium citrate was used to model NTBI. Ferric nitrilotriacetate (Fe-NTA) was used to saturate transferrin. Total cellular iron was assayed by ferrozine. The level of cytosolic reactive oxygen species (ROS), tested using 2,7-dichlorofluorescein diacetate (H_2DCF-DA), was calculated from slopes of fluorescence-versus-time data. Detailed methods are provided in the **Supplement**.

Statistics

Continuous data was presented as mean±SD or median±interquartile range and compared using the t-test or nonparametric tests, depending on assumed distribution, unless otherwise specified. Categorical variables were compared using χ^2-test. A $p<0.05$ was statistically significant.

Results

Factors associated with MH.
To determine factors associated with MH, biomarkers were compared in transfusion-dependent thalassemia patients with (n=24) and without (n=49) MH. The sTfR1 emerged as the factor most significantly associated with MH ($p<0.001$, **Figure 1A-C**) being >3-fold higher in controls than in MH (medians 4.06 vs. 1.26µg/mL, p=0.0005) with an area-under-curve for the receiver operating characteristic curve (AUC_{ROC}) of 0.8, p=0.0004. A threshold of 1.77µg/mL was predictive of MH with 89.7% sensitivity, 64.7% specificity (normal range for sTfR1: 0.3-1.65µg/mL). Other biomarkers significantly associated with MH were bilirubin, reticulocyte count, hepcidin, LIC, and serum ferritin (**Table 1).** Although median LPI differed insignificantly between MH and non-MH patients, a cut-off threshold of >0.31µM was significantly associated with MH (χ^2 p=0.04). Differences in NTBI, LPI, transferrin saturation (TfSat), and transfusion iron load rate (ILR) were insignificant (**Figure 1D-G)**, and no such thresholds were found for NTBI or TfSat.

High liver iron concentration and, to a lesser extent, serum ferritin are also significant risk factors for MH in our study, which is of interest, as this was not seen in earlier studies[33]. However, liver iron determination in earlier studies was not optimal[34] and many patients had recently undergone intesive iron chelation which removes iron faster from the liver than from the heart[35], thereby obscuring such a relationship[36]. A further significant, though weak, risk factor for MH was high plasma hepcidin. Hepcidin did not correlate with markers of iron overload such as LIC (as hepatic R2*, p=0.4), or ferritin (p=0.52), but inversely correlated significantly to sTfR1 (Spearman r=-0.54, $p<0.0001$). sTfR1 did not correlate with LIC or ferritin (p=0.4 and 0.52, respectively; **Supplement Figure 1**). Insignificant MH associations were with nucleated red cells, total serum iron, age, weight, ILR, TfSat, and GDF-15.

Relationship of transferrin-iron utilization to MH in transfusion-dependent thalassemia.
To gain insight into the relationship between MH and sTfR1, we utilized understandings from ferrokinetic studies[29,30] which established the erythron transferrin uptake (ETU) as proportional to plasma sTfR1. The regression equation (r^2=0.84) for ETU was calculated from published data[29]:

ETU[µmol Fe/L plasma/day]=0.013*sTfR1[µg/L]+2.25

Assuming that the relationship remains temporally stable, sTfR1 represents erythropoiesis quantitatively, given that plasma levels are proportionate to tissue transferrin receptors of the whole organism[31], of which erythroid cells are the main *dynamic* component. ETU can be expressed as a rate corrected for estimated blood volume: BV=70mL/kg (males), 65mL/kg (females), and patient weight (erythroid transferrin uptake rate, ETUR).

ETUR[mg/kg/d]=ETU[µmol/L/d]*55.845[g/mol]/1000*BV[mL]/1000/weight[kg].

Although transfusion does not directly relate to cardiac iron, when plasma sTfR1 levels were expressed as ETUR (i.e. transferrin-iron utilization rate) and compared

to the transfusion ILR (**Figure 2A-C**), MH was present only when the 'net ILR' (ILR-ETUR) exceeded 0.21mg/kg/d ($p<0.001$). Above and below this threshold, LIC[34], TfSat, and NTBI were similar (9.7 vs. 10.1 mg/g dry weight, 96 vs. 98%, 3 vs. 2.6μM, p=ns), while LPI was >3-fold higher (0.35 vs. 0.1 μM, p=0.01). Thus, LPI was high only in patients where the net ILR exceeded 0.21mg/kg/d, whereas LIC, TfSat, NTBI showed no difference between patients with and without MH, even when adjusted for the net ILR **(Figure 2C**).

This suggests a link between iron clearance from transferrin -- a process implying the formation of transient levels of apotransferrin -- and the low propensity to MH in transfusion-dependent thalassemia. We hypothesized that increased transient local concentrations of apotransferrin in the marrow and circulating reticulocytes[37] could decrease the uptake of NTBI into the myocardium. With similar TfSat and NTBI in MH-positive and MH-negative patients, this effect of recycled apotransferrin was expected to influence the speciation of NTBI.

Effects of iron-to-citrate ratio on iron detection in the LPI assay

As LPI was found to differ between MH-positive and MH-negative patients, we wished to characterise which fraction of NTBI was detected by the LPI assay. In particular, we wished to determine whether LPI was most detectable under conditions where either monomer or oligomer ferric citrate species predominated. In **Figure 3A** at constant citrate concentrations (100μM), the proportion of iron detectable in the LPI assay decreases as iron concentration increases. Conversely, LPI is proportionately most detectable at 1000-fold citrate excesses. Under these clinically relevant conditions, the citrate excess favors the formation of monomer rather than oligomer species. As LPI was associated with an increased MH risk in our clinical observations, these findings suggest that the monomer LPI might be the species most readily taken into myocardial cells.

Effect of iron-to-citrate ratio on iron uptake into HL-1 cardiomyocytes

To confirm this interpretation, we examined iron uptake in HL-1 cardiomyocytes at varying iron-to-citrate ratios. In **Figure 3B** the effect of increasing ferric iron at constant citrate concentration (100μM) on HL-1 uptake is shown at 24h. A clear plateau effect is seen whereby iron uptake does not increase further when citrate exceeds iron by less than 100-fold. Under these conditions oligomer rather than monomer ferric citrate species are favored[17]. This suggests that oligomer iron citrate species are less available for uptake by cardiomyocytes than the monomer species.

Effect of iron-to-citrate ratio on iron binding to transferrin

We wished to determine how the iron-to-citrate ratio also affected the availability of ferric iron to bind transferrin. In **Figure 3C**, apotransferrin (at 35.5μM or 71μM iron binding equivalents, IBE) was incubated with buffered ferric citrate at 0 to 4000-fold citrate excess. Iron binding to transferrin, determined by spectroscopy, increased to a maximum of 40% as the citrate excess increased. Thus under conditions favoring monomer ferric citrate species, binding of iron to transferrin is more rapid than where oligomers predominate.

Low (nanomolar) concentration of apotransferrin substantially decreases LPI

The preferential binding of the monomer ferric citrate species by transferrin was predicted to decrease those same species responsible for activity in the LPI assay. We tested this in **Figure 3D**, where the control without transferrin showed increasing LPI values with increasing ferric iron concentration (at constant 100µM citrate). When apotransferrin is added at remarkably low concentrations (30nM or 60nM IBE), LPI detectability is decreased substantially across all ratios. This effect exceeds results expected from simple stoichiometric binding. Higher concentration of apotransferrin (10µM) completely abrogates LPI detectability up to 10µM iron. These findings show that the redox-active iron species responsible for the majority of LPI detectability is present at a very low concentration (nanomolar). This species is most likely to be ferric monocitrate because apotransferrin is known to bind ferric monocitrate most avidly.

Effect of apotransferrin on HL-1 *cardiomyocyte iron uptake from ferric citrate species*

Having established the conditions favoring LPI detectability and apotransferrin binding of ferric citrate species, we wanted to test whether these same conditions are those that most inhibit iron uptake in HL-1 cardiomyocyte cells.

We first examined the effect of transferrin on uptake from ferric ammonium citrate (FAC), which is a stable form of monomeric ferric iron coordinated by two citrate molecules[38]. In **Figure 3E** it can be seen that iron uptake from 1µM FAC is almost completely inhibited by apotransferrin at 1µM (2µM iron binding equivalents). In **Figure 3F**, the effect of constant transferrin concentration with varying percentage saturations on iron uptake from 5µM FAC at 24h is examined. Uptake is completely inhibited by physiologically relevant transferrin concentrations of 37µM (74µM iron-binding equivalents) at saturations below 99%.

We then wished to examine the inhibitory effect of apotransferrin on iron uptake at varying iron-to-citrate ratios. In order to study short-time intervals, we developed an intracellular ROS assay and validated this against total cellular iron at 24h (**Figure 4A**). The control iron uptake marked by intracellular ROS at 60 minutes in **Figure 4B** (closed circles) shows a plateau, as previously noted for total iron uptake at 24h (**Figure 3B**). Thus, under conditions where oligomer species increasingly predominate, uptake into HL-1 cells forms a plateau. In the same experiment (**Figure 4B** triangles**)**, the addition of 5µM apotransferrin inhibits uptake up to the point where ferric citrate approaches 10µM, at which concentration iron uptake exceeds that from control. Importantly, this contrasts with the effects of apotransferrin on iron uptake from FAC (**Figure 3F)** where uptake was inhibited at every apotransferrin concentration. The key difference between **Figures 3B, E and F** is the form of iron citrate presented to the cells. Freshly prepared FAC is a fully co-ordinated monomeric iron dicitrate[38], whereas at the 1:10 iron-to-citrate ratio used in **Figure 3B**, mixtures of oligomer and monomer iron species are present[17,16].

The increased uptake for apotransferrin in **Figure 4B** might be interpreted superficially as increased uptake from holotransferrin, formed from the addition of apotransferrin to iron citrate. However control experiments, including **Figure 4C**

and **Supplement Figure 2**, show that incubation of HL-1 cardiomyocytes with holotransferrin does not increase iron uptake: increasing concentration of 95%-saturated transferrin actually inhibited iron accumulation.

An alternative explanation for the findings in **Figure 4B** is that the interaction of apotransferrin with iron citrate alters the proportions of citrate species. To test this hypothesis further, we examined in **Figure 4D** the iron uptake at increasing concentrations of apotransferrin but constant iron citrate concentrations that favor oligomer species (10μM ferric iron and 100μM citrate). Apotransferrin between 1 and 8μM increased iron uptake but at higher apotransferrin concentrations (8μM or 16μM) uptake was inhibited. This is more consistent with catalytic depolymerisation of oligomers to monomers as elaborated in the discussion.

We suggest therefore that the presence of apotransferrin in **Figures 4B** and **D** favors the formation of citrate species that are more rapidly taken into cells, namely monomeric iron species. Only when the iron binding capacity of apotransferrin exceeds the iron content of the ferric citrate (here above about 10μM), is iron uptake inhibited. We conclude that speciation of iron citrate is critical to cardiomyocyte iron uptake and that apotransferrin alters this speciation.

Discussion

In this paper we have sought to identfy risk factors for MH in transfused thalassemia patients. A key novel finding is that low levels of sTfR1 appear a powerful predictor for MH with an odds ratio of 21. It is unlikely that sTfR1 exerts a direct mechanistic role in iron distribution, as mice transfected with sTfR1 showed similar iron absorption and hepcidin to controls[39]. Furthermore, circulating concentration of sTfR1 (nanomolar) is three logs less than that of diferric transferrin and thus unlikely to be a significant receptor trap for transferrin iron utilisation. We also found a clear relationship between the transfusion-iron loading rate and the myocardial iron by MRI (mR2*) in MH(+) patients (**Figure 2B**). This suggested that the balance between the transfusion iron-loading rate and erythron iron utilization might be key to MH. We therefore developed a model building on data linking sTfR1 to quantitate iron utilization by the erythron (the ETUR)[29,30], and found that the difference between the ILR and the ETUR predicted MH with an odds ratio of 48. We identified a threshold for this difference of 0.21mg/kg/day, above which MH was more likely and below which MH was not seen (**Figure 2C**), even in the presence of high total body iron (**Figure 2D**). Hence a high transfusion iron intake relative to endogenous erythropoiesis puts patients at increased risk of MH.

The high transfusion iron intake relative to endogenous erythropoiesis as a risk for MH is supported by other clinical observations. Additional factors that we found correlated with lower MH risk, such as high bilirubin and high reticulocytes, are also consistent with a high activity of the erythron. Others have shown that reticulocyte count below 5% in sickle cell disease was actually found to predict premature development of cardiac iron deposition[40]. Erythropoietin, although not measured in this cohort, would be predicted to negatively correlate with MH because it drives sTfR1 levels[29] and correlates with them closely in transfusion-

dependent thalassemia. The relationship of the age of onset of transfusion dependence to MH suggests that an initial expansion of the bone marrow, by under-transfusion or late introduction of transfusion, is hard to suppress even after many subsequent years of hypertransfusion (**Supplement Figure 3**). Others have indirectly linked the absence of MH with extramedullary hematopoiesis in transfused thalassemia patients, using extramedullary masses by MRI as surrogate markers of erythroid mass[41], which also proves the point that even life-long hypertransfusion does not suppress erythropoiesis completely. A high risk of MH has also been identified in another transfusion-dependent condition with low iron utilisation and extremely low sTfR1, namely Diamond-Blackfan anemia[23,42]. Conversely, non-transfusion-dependent thalassemia patients have very high sTfR1 levels[13] with high ineffective erythropoiesis but a low risk of MH[43,44], despite substantial iron overload. Factors in addition to iron uptake may influence net MH. For example, our findings of increased plasma hepcidin in MH-positive patients are consistent with recent work in animal models of iron overload implicating iron exit through cardiac ferroportin channels as important to myocardial iron retention[45,46]. There was a significant relationship between hepcidin and sTfR1, but not with GDF15, nonetheless it would be of value to look at this relationship with erythroferrone when the assay becomes available.

What is the role of the labile plasma iron fraction of NTBI in MH risk? A notable feature of non-transfusion-dependent thalassemias, reported elsewhere on a large cohort of 155 patients, is that, even in the presence of high levels of body iron and raised NTBI, LPI is typically within the normal range, while the few cases with increased LPI have no apotransferrin[13]. This is consistent with this paper's findings in trasfusion-dependent patients where a >3-fold difference in LPI was seen across the ILR-ETUR threshold, while plasma NTBI levels and transferrin saturations were indistinguishable (**Figure 2C**). This suggests that LPI-detectable species are those taken up by cardiomyocytes, consistent with previous clinical observations linking LPI-detectable iron to MH[21].

As the LPI assay detects only the redox-active sub-fraction of NTBI, we wished to determine whether LPI-detectable NTBI species were those particularly prone to cardiomyocyte uptake. We used buffered ferric citrate as a model for NTBI at constant citrate of 100μM to represent plasma concentration. Detectability of iron by the LPI assay was less using iron citrate as the source of iron than Fe-NTA (**Supplement Figure 4**), indicating that only a proportion of ferric citrate species are detectable by the LPI assay. Furthermore, LPI was proportionately most detectable when citrate exceeded ferric iron concentrations by >100-fold; ratios known to be associated with the appearance of monoferric citrate species[17,16]. We therefore hypothesised that monoferric species are taken into cardiomyocytes most readily since, in our study, MH associates with LPI, rather than with total NTBI. Monoferric species include ferric monocitrate and ferric dicitrate[17,16] (**Figure 5,** compounds A and C). Redox-cycling of iron species is dependent on the ability of reductants and oxidants to gain access to the iron center by displacing the monodentate water molecules which occupy the ‘free’ coordination sites of iron complex that is only partially coordinated by ligands such as one tridentate citrate molecule or one bidentate deferiprone molecule[22] (**Figure 5**, coordination sites in bold). Ferric dicitrate, with its iron center fully hexa-co-ordinated by two tridentate citrate molecules, has a high stability constant for iron(III)[16], is less redox-active[22],

thus less of a candidate for uptake (a process requiring reduction[14,47,48]). We predicted therefore that it is ferric monocitrate which is most available to cardiomyocyte uptake as well as to transferrin binding, as discussed below.

We found that the cardiomyocyte iron uptake from citrate and its inhibition by apotransferrin are speciation-dependent. Cardiomyocyte uptake of ferric citrate indeed occurred most rapidly where citrate excess was high (**Figure 3B**), under conditions favoring monomer rather than oligomer species. This contrasts with previous reports for hepatocytes and cardiomyocytes[8,47,49] using Fe-NTA, a non-physiological but typically monomeric iron source, where the speciation dependence of uptake was not studied.

Very low concentration of apotransferrin, and transferrin saturations ≤99% inhibited cardiomyocyte iron uptake from ferric ammonium citrate (**Figures 3E** and **F**). This suggests that the NTBI species partaking in cardiac uptake constitute only a small fraction of the total NTBI. The small magnitude of this fraction is consistent with monocitrate being the predominant species for cardiomyocyte iron uptake. Furthermore, because apotransferrin decreases LPI in our assays, and iron monocitrate is the species most rapidly chelated by apotransferrin, as described above, ferric monocitrate is most likely the predominant LPI species. Very low transferrin concentrations (nanomolar) were all that were necessary to inhibit LPI-detectable iron citrate species (**Figure 3D**), which we identified above as being monoferric citrate. This suggests that this LPI-detectable species is present at very low concentration but is kinetically labile.

Surprisingly, we found that at very high ferric citrate concentrations (10μM, **Figure 4D**), under conditions that favor oligomer species, rarely observed clinically, sub-stoichiometric concentrations of apotransferrin, insufficient to bind all the ferric citrate, actually increased cellular iron uptake. This is not due to increased uptake by holotransferrin, as negligible iron was delivered to cardiomyocytes by holotransferrin (**Figure 4C**), consistent with previous observations in cardiomyocytes[8]. We deduced therefore that increased uptake from ferric citrate in the presence of apotransferrin under these conditions may occur by accelerating the dissociation of oligomer to monomer citrate species (**Figure 5**). This deduction is consistent with the observation that the transition from absence to excess of transferrin binding capacity is associated with the generation of kinetically labile iron citrate species that are rapidly taken into HL-1 cardiomyocytes (**Figure 4D**). This effect is notable only when apotransferrin is present at intermediate concentrations allowing depolymerisation of oligomers to their constituent monomers (i.e. ferric monocitrate, see **Figure 5**). Previous work, consistent with this model, showed that the rate-limiting step for exchange of polymeric ferric citrate iron with apotransferrin was the de-polymerization and release of monomeric (mononuclear) ferric citrate[50]. Ferric dicitrate was unreactive towards apotransferrin unless converted to an active intermediate, which the authors had supposed to be the monocitrate[50]. Importantly, such conditions of very high NTBI are unlikely to occur clinically so that inhibitory effects of apotransferrin on NTBI uptake will predominate.

In conclusion, we propose a mechanism of MH inhibition by the generation of apotransferrin during erythropoiesis. Taken together our clinical and *in vitro* data point to increased generation of apotransferrin by an active bone marrow (marked by high

sTfR1) as a key mechanism for decreasing the MH risk in transfusion-dependent thalassemias. We suggest that a local excess of apotransferrin in the bone marrow, around sinusoids and reticulocytes, chelates monomeric ferric citrate species, the same species most rapidly taken into the myocardium. The clinical implications of this are that a critical balance appears here to exist between the transfusion rate, endogenous erythropoiesis, MH risk and NTBI speciation. We suggest that prospective longitudinal data collection, including sequential sTfR1 measurement, would be valuable so that clear recommendations could be made about whether reducing transfusion exposure decreases the MH risk. Furthermore, due to the marked geographic variability in MH risk[7] that cannot be related solely to chelation practices, cross-sectional studies on the impact of regional transfusion policies on ETUR and MH risk could be indicated.

References

1. Borgna-Pignatti C, Cappellini MD, De Stefano P, et al. Survival and complications in thalassemia. Ann N Y Acad Sci. 2005;1054:40–47.
2. Olivieri NF, Nathan DG, MacMillan JH, et al. Survival in medically treated patients with homozygous beta-thalassemia. N Engl J Med. 1994;331(9):574–578.
3. Telfer PT, Prestcott E, Holden S, Walker M, Hoffbrand AV, Wonke B. Hepatic iron concentration combined with long-term monitoring of serum ferritin to predict complications of iron overload in thalassaemia major. Br J Haematol. 2000;110(4):971–977.
4. Gabutti V, Piga A. Results of long-term iron-chelating therapy. Acta Haematol. 1996;95(1):26–36.
5. El Beshlawy A, El Tagui M, Hamdy M, et al. Low prevalence of cardiac siderosis in heavily iron loaded Egyptian thalassemia major patients. Ann Hematol. 2014;93(3):375–379.
6. Pennell DJ, Berdoukas V, Karagiorga M, et al. Randomized controlled trial of deferiprone or deferoxamine in beta-thalassemia major patients with asymptomatic myocardial siderosis. Blood. 2006;107(9):3738–3744.
7. Aydinok Y, Porter JB, Piga A, et al. Prevalence and distribution of iron overload in patients with transfusion-dependent anemias differs across geographic regions: Results from the CORDELIA study. Eur J Haematol. 2015;95(3):244–253.
8. Liu Y, Parkes JG, Templeton DM. Differential accumulation of non-transferrin-bound iron by cardiac myocytes and fibroblasts. J Mol Cell Cardiol. 2003;35(5):505–514.
9. Singh S, Hider RC, Porter JB. A direct method for quantification of non-transferrin-bound iron. Anal Biochem. 1990;186(2):320–323.
10. Garbowski MW, Ma Y, Fucharoen S, Srichairatanakool S, Hider R, Porter JB. Clinical and methodological factors affecting non-transferrin-bound iron values using a novel fluorescent bead assay. Transl Res. 2016;177:19–30.e5.
11. Esposito BP, Breuer W, Sirankapracha P, Pootrakul P, Hershko C, Cabantchik ZI. Labile plasma iron in iron overload: Redox activity and susceptibility to chelation. Blood. 2003;102(7):2670–2677.
12. Gosriwatana I, Loreal O, Lu S, Brissot P, Porter J, Hider RC. Quantification of non-transferrin-bound iron in the presence of unsaturated transferrin. Anal Biochem. 1999;273(2):212–220.
13. Porter J, Cappellini M, Kattamis A, et al. Iron overload across the spectrum of non-transfusion-dependent thalassaemias: role of erythropoiesis, splenectomy and transfusion. Br J Haematol. 2017;176: 288–299.
14. Oudit GY, Sun H, Trivieri MG, et al. L-type Ca^{2+} channels provide a major pathway for iron entry into cardiomyocytes in iron-overload cardiomyopathy.

Nat Med. 2003;9(9):1187–1194.

15. Fernandes JL, Loggetto SR, Veríssimo MPA, et al. A randomized trial of amlodipine in addition to standard chelation therapy in patients with thalassemia major. Blood. 2016;128(12):1555–1561.

16. Silva AM, Kong X, Parkin MC, Cammack R, Hider RC. Iron(III) citrate speciation in aqueous solution. Dalt Trans. 2009;(40):8616–8625.

17. Evans RW, Rafique R, Zarea A, et al. Nature of non-transferrin-bound iron: Studies on iron citrate complexes and thalassemic sera. J Biol Inorg Chem. 2008;13(1):57–74.

18. Silva AM, Hider RC. Influence of non-enzymatic post-translation modifications on the ability of human serum albumin to bind iron. Implications for non-transferrin-bound iron speciation. Biochim Biophys Acta. 2009;1794(10):1449–1458.

19. Evans P, Kayyali R, Hider RC, Eccleston J, Porter JB. Mechanisms for the shuttling of plasma non-transferrin-bound iron (NTBI) onto deferoxamine by deferiprone. Transl Res. 2010;156(2):55–67.

20. Zanninelli G, Breuer W, Cabantchik ZI. Daily labile plasma iron as an indicator of chelator activity in Thalassaemia major patients. Br J Haematol. 2009;147(5):744–751.

21. Wood JC, Glynos T, Thompson A, et al. Relationship between labile plasma iron, liver iron concentration and cardiac response in a deferasirox monotherapy trial. Haematologica. 2011;96(7):1055–1058.

22. Devanur LD, Neubert H, Hider RC. The fenton activity of iron(III) in the presence of deferiprone. J Pharm Sci. 2008;97(4):1454–1467.

23. Porter JB, Walter PB, Neumayr LD, et al. Mechanisms of plasma non-transferrin bound iron generation: Insights from comparing transfused diamond blackfan anaemia with sickle cell and thalassaemia patients. Br J Haematol. 2014;167(5):692–696.

24. Cohen AR, Glimm E, Porter JB. Effect of transfusional iron intake on response to chelation therapy in β-thalassemia major. Blood. 2008;111(2):583–587.

25. Taher AT, Porter J, Viprakasit V, et al. Deferasirox reduces iron overload significantly in nontransfusion-dependent thalassemia: 1-Year results from a prospective, randomized, double-blind, placebo-controlled study. Blood. 2012;120(5):970–977.

26. Gkouvatsos K, Papanikolaou G, Pantopoulos K. Regulation of iron transport and the role of transferrin. Biochim Biophys Acta - Gen Subj. 2012;1820(3):188–202.

27. Hikawa A, Nomata Y, Suzuki T, Ozasa H, Yamada O. Soluble transferrin receptor-transferrin complex in serum: Measurement by latex agglutination nephelometric immunoassay. Clin Chim Acta. 1996;254(2):159–172.

28. Ponka P, Lok CN. The transferrin receptor: role in health and disease. Int J Biochem Cell Biol. 1999;31(10):1111–1137.

29. Beguin Y, Clemons GK, Pootrakul P, Fillet G. Quantitative assessment of erythropoiesis and functional classification of anemia based on measurements of serum transferrin receptor and erythropoietin. Blood. 1993;81(4):1067–1076.

30. Huebers HA, Beguin Y, Pootrakul P, Einspahr D, Finch CA. Intact transferrin receptors in human plasma and their relation to erythropoiesis. Blood. 1990;75(1):102–107.

31. R'zik S, Beguin Y. Serum soluble transferrin receptor concentration is an accurate estimate of the mass of tissue receptors. Exp Hematol. 2001;29(6):677–685.

32. Cazzola M, De Stefano P, Ponchio L, et al. Relationship between transfusion regimen and suppression of erythropoiesis in beta-thalassaemia major. Br J Haematol. 1995;89(3):473–478.

33. Anderson LJ, Holden S, Davis B, et al. Cardiovascular T2-star (T2*) magnetic resonance for the early diagnosis of myocardial iron overload. Eur Heart J. 2001;22(23):2171–2179.

34. Garbowski MW, Carpenter JP, Smith G, et al. Biopsy-based calibration of T2* magnetic resonance for estimation of liver iron concentration and comparison with R2 Ferriscan. J Cardiovasc Magn Reson. 2014;16(1):40.

35. Anderson LJ, Westwood MA, Holden S, et al. Myocardial iron clearance during reversal of siderotic cardiomyopathy with intravenous desferrioxamine: A prospective study using T2* cardiovascular magnetic resonance. Br J Haematol. 2004;127(3):348–355.

36. Noetzli LJ, Carson SM, Nord AS, Coates TD, Wood JC. Longitudinal analysis of heart and liver iron in thalassemia major. Blood. 2008;112(7):2973–2978.

37. Finch C, Huebers H, Eng M, Miller L. Effect of transfused reticulocytes on iron exchange. Blood. 1982;59(2):364–369.

38. Matzapetakis M, Raptopoulou CP, Tsohos A, Papaefthymiou V, Moon N, Salifoglou A. Synthesis, Spectroscopic and Structural Characterization of the First Mononuclear, Water Soluble Iron−Citrate Complex, $(NH_4)_5Fe(C_6H_4O_7)_2 \cdot 2H_2O$. J Am Chem Soc. 1998;120(10):13266–13267.

39. Flanagan JM, Peng H, Wang L, et al. Soluble transferrin receptor-1 levels in mice do not affect iron absorption. Acta Haematol. 2006;116(4):249–254.

40. Meloni A, Puliyel M, Pepe A, Berdoukas V, Coates TD, Wood JC. Cardiac iron overload in sickle-cell disease. Am J Hematol. 2014;89(7):678–683.

41. Ricchi P, Meloni A, Spasiano A, et al. Extramedullary hematopoiesis is associated with lower cardiac iron loading in chronically transfused thalassemia patients. Am J Hematol. 2015;90(11):1008–1012.

42. Wood JC. Cardiac iron across different transfusion-dependent diseases. Blood Rev. 2008;22(SUPPL. 2):14–21.

43. Taher AT, Musallam KM, Wood JC, Cappellini MD. Magnetic resonance evaluation of hepatic and myocardial iron deposition in transfusion-

independent thalassemia intermedia compared to regularly transfused thalassemia major patients. Am J Hematol. 2010;85(4):288–290.

44. Roghi A, Cappellini MD, Wood JC, et al. Absence of cardiac siderosis despite hepatic iron overload in Italian patients with thalassemia intermedia: an MRI T2* study. Ann Hematol. 2010;89(6):585–589.

45. Lakhal-Littleton S, Wolna M, Carr CA, et al. Cardiac ferroportin regulates cellular iron homeostasis and is important for cardiac function. Proc Natl Acad Sci U S A. 2015;112(10):3164–3169.

46. Altamura S, Kessler R, Groene HJ, et al. Resistance of ferroportin to hepcidin binding causes exocrine pancreatic failure and fatal iron overload. Cell Metab. 2014;20(2):359–367.

47. Parkes JG, Olivieri NF, Templeton DM. Characterization of Fe^{2+} and Fe^{3+} transport by iron-loaded cardiac myocytes. Toxicology. 1997;117(2–3):141–151.

48. Liuzzi JP, Aydemir F, Nam H, Knutson MD, Cousins RJ. Zip14 (Slc39a14) mediates non-transferrin-bound iron uptake into cells. Proc Natl Acad Sci U S A. 2006;103(37):13612–13617.

49. Parkes JG, Randell EW, Olivieri NF, Templeton DM. Modulation by iron loading and chelation of the uptake of non-transferrin-bound iron by human liver cells. Biochim Biophys Acta. 1995;1243(3):373–380.

50. Bates GW, Billups C, Saltman P. The Kinetics and Mechanism of Iron(III) Exchange between Chelates and Transferrin. I. THE COMPLEXES OF CITRATE AND NITRILOTRIACETIC ACID. J Biol Chem. 1967;242(12):2810–2815.

Tables

Table 1. Significant clinical and laboratory variables associated with MH in TDT.

variables	threshold	OR±SE	p value	MH(-)	MH(+)	p-value
Chelation start age [yr]	≥7.5	8.42±0.81	0.009	7.5 (3.5-12)	2.5 (2-6)	0.0039
Age [yr]	≥35.92	5.9±0.61	0.005	35.67 ± 10.57	32.11 ± 6.92	0.12
Un-chelated transfusion years [%]	≥5	4.68±0.6	0.018	8 (3-18)	4.5 (3-9)	0.15
Transfusion dependency start age [yr]	≥1.5	3.64±0.58	0.046	1.5 (0.67-5.5)	0.9 (0.5-1.88)	0.02
ETUR-ILR [mg/kg/d]	<0.21	48.4±1.15	0.00008	0.09 (-0.08-0.17)	0.27 (0.24-0.34)	0.0002
Total bilirubin [µM]	≥16.5	21±1.1	0.0014	35 (25-52)	22 (14-29.75)	0.0004
Hepatic R2* [s^{-1}]	<142[1]	21±1.06	0.0007	139 (79-365)	326 (235-625)	0.003
sTfR1 [mg/mL]	≥1.34	20.81±0.87	0.00016	4.06 (2.55-5.95)	1.26 (0.68-2.71)	0.0003
ETU [mgFe/L whole blood/day]	≥1.45	16.04±0.73	0.0001	14.06 (6.53-18.26)	3.89 (1.82-4.86)	0.0001
Absolute reticulocyte count [$\times 10^9$/L]	≥7.4	13.75±1.14	0.02	44.4 (19.95-128.9)	20.6 (7.1-30.7)	0.029
LPI [µM]	<0.31	10.5±1.02	0.04	0.1 (0.02-0.17)	0.27 (0.05-0.45)	0.13
Hepcidin [nM]	<6.78	9±0.81	0.006	6.8 (3.18-22.13)	14.3 (7.58-23.65)	0.04
Ferritin [µg/L]	<1700	7.63±0.62	0.001	1309 (844-3057)	2926 (1958-4284)	0.0013

Medians with 25th-75th percentile range or mean ± SD are provided for MH(-) and MH(+) groups, compared with Mann-Whitney or t-test, as well as threshold protecting from MH and its odds ratio (OR). [1]LIC=4.41mg/g dry weight[34]. [yr]=years.

Figure legends

Figure 1. Biomarkers in patients with and without myocardial siderosis. Comparison of means and medians in patients with and without cardiac iron, MH(+) and MH(-), respectively, shown as box and whisker (min-max) plots. (A) Soluble transferrin receptor-1, sTfR1: 4.06 vs. 1.26µg/mL, MW p=0.0005. (B) Receiver operating characteristic (ROC) curve for sTfR1, AUC_{ROC}=0.8±0.07 (p=0.0004). (C) Plot of cardiac R2* vs. sTfR1, Spearman correlation coefficient r = –0.61, p<0.0001. (D) Non-transferrin-bound iron, NTBI: 2.86 vs. 2.7µM, MW p=0.59. (E) Transferrin saturation, TfSat: 100 vs. 100%, MW p=0.94. (F) Labile plasma iron, LPI: 0.1 vs. 0.27µM, MW p=0.13. (G) Transfusion-iron load rate, ILR: 0.32 vs. 0.35mg Fe/kg/day, t-test p=0.19. (H) Growth-differentiation factor-15, GDF15: 6702 vs. 4430pg/mL, MW p=0.4 (I) Plasma hepcidin 6.8 vs. 14.3nM, MW p=0.04. MW, Mann-Whitney test; AUC, area under curve, MH, myocardial hemosiderosis.

Figure 2. Balance between transfusion-iron load rate and erythroid transferrin uptake rate derived from sTfR1 relates to cardiac iron. (A) Cardiac R2* plotted against transfusion-iron load rate, grey circles mark patients with cardiac iron ($cR2^*>50s^{-1}$), open circles – patients without cardiac iron; no relationship overall. (B) Cardiac R2* (cR2*) plotted against transfusion-iron load rate (ILR), open circles mark patients with cardiac iron ($cR2^*>50s^{-1}$), grey circles – patients without cardiac iron; no relationship overall, relationship present in patients with cardiac iron only, r^2=0.61; points differ in size accoding to sTfR1 level [µg/mL], see inset. (C) same as in panel B but the *x*-axis shows ILR corrected for utilisation rate derived from sTfR1 according to *Beguin et al 1993*[29] (ETU[µmol/L/day]=0.013×sTfR1 [ug/L]+2.25; ETUR[mg/kg/d]=ETU×55.845[g/mol]/1000×Blood Volume[mL]/1000/body weight[kg]). Highly discriminant threshold 0.21mg/kg/d p<0.0001, 100% sensitive, 83% specific for MH (PPV 71%, NPV 100%) above and below which the LIC, TfSat and NTBI do not differ (p=ns) but LPI is 0.35µM vs. 0.1 µM p=0.01, respectively. (D) same as panel C but points differ in size according to total body iron derived from LIC values.

Figure 3. Effect of ferric citrate speciation on LPI detectability, total cellular iron and transferrin binding. (A) LPI as a percentage of ferric citrate with constant citrate (100µM) and variable iron (0-10µM, shown next to data points in µM), as a function of excess citrate (fold), representative of 3 experiments. This illustrates what proportion of a given ratio species is LPI-detectable. (B) Total cellular iron dose response in confluent HL-1 cells to 24h incubation in Claycomb medium (CM) with ferric citrate in MOPS pH=7.4 at variable Fe:citrate ratios and constant citrate at 100µM, r^2=0.95, EC_{50}=0.31µM, EC_{90}=1.09µM; shown as mean±SD, n=6. (C) Percentage of ferric citrate iron that binds to 35.5µM apotransferrin (ApoTf) to form ferrotransferrin (over 2h incubation at 37°C) as a function of citrate:Fe ratio. 0-30µM iron and 100µM citrate were increased 25.5-fold to keep the same ratio (see legend: 0-765µM and 2550µM f.c. respectively) in order to better resolve absorbance peaks of holotransferrin formation (at 465nm, inset), and compared to 35.5µM 100% saturated ferrotransferrin absorbance of 1.69. Percentage of iron bound to transferrin was calculated from transferrin iron content/nominal concentrations prepared (see inset, mean±SD, n=2). (D)

Apotransferrin-dependent inhibition of LPI in ferric citrate. Apotransferrin (ApoTf) with 25mM bicarbonate was added at 0-10µM (f.c.) together with ferric citrate, subsequent DHR oxidation was followed up for 1 hour. LPI values are interpolated from the standard curve, mean±SD, n=3. (E) HL-1 cells grown to confluence and incubated for 24h in CM with 1µM ferric ammonium citrate (FAC) ±0-2.5µM ApoTf; ANOVA $p<0.001$, mean±SD, n=2, Bonferroni post-test significant for ApoTf effect in the FAC group. Global fit $r^2=0.91$, ApoTf $IC_{50}=0.81$µM, curves significantly different ($p<0.0001$). (F) Transferrin saturation-dependent model of NTBI uptake (as FAC) into HL-1 cells grown to confluence then incubated in CM with apotransferrin and 100% saturated holotransferrin at relevant ratios to obtain a 37.5µM TfSat model ±5µM FAC; difference vs. control (no NTBI) only detectable for TfSat=100%, i.e. when no apotransferrin is present (multiple t-test with Holm-Sidak correction for multiple comparisons, $p=0.004$, mean±SD, n=6).

Figure 4. Effect of apotransferrin and citrate speciation on the iron uptake marked by cytosolic ROS. (A) The relationship of intracellular ROS levels by the DCF method and the total cellular iron by the ferrozine method, $r=0.91$, $p<0.0001$; Deming regression slope $1.14\times10^{-5}\pm1.68\times10^{-6}$, intercept $2.69\times10^{-5}\pm5.08\times10^{-6}$, mean±SD, n=6. (B) Cytosolic ROS levels in HL-1 cardiomyocytes as a function of control ferric citrate (iron 0-30µM, citrate 100µM) in MOPS pH=7.4 with (triangles) and without (circles) 5µM apotransferrin (ApoTf) in 25mM bicarbonate; mean±SD, n=5. (C) Dose response of cytosolic ROS levels in HL-1 cardiomyocytes to 95% saturated transferrin (0.37-15µM) ±100µM iron-binding equivalents of CP40, an extracellular chelator, mean±SD, n=4. (D) Cytosolic ROS formation in HL-1 cardiomyocytes showing recent uptake of iron from predominantly oligomer species (10µM iron, 100µM citrate) or control (citrate only) under dose response effect of 0-16µM apotransferrin in 30mM bicarbonate/PBS; mean±SD, n=4.

Figure 5. Model of apotransferrin-dependent re-speciation of polymeric ferric citrate.
The paradoxical effect of apotransferrin seen in Figure 4D where uptake from 10µM ferric citrate is increased before it is abolished by apotransferrin, is consistent with the sub-equivalent concentration of apotransferrin disrupting ferric citrate oligomers and releasing from them ferric monocitrate species. As apotransferrin binds a portion of iron in high ratio ferric citrate, this decreases the amount of iron per citrate, so effectively changes the iron-to-citrate ratio, i.e. re-speciates it. In the presence of apotransferrin and bicarbonate, which forms a ternary complex with citrate, oligomer complexes of ferric citrate become a source of ferric monocitrate species. These are subject to competition with uptake mechanisms for cellular entry (dotted line), with apotransferrin for the formation of ferrotransferrin and with citrate for the formation of ferric dicitrate, citrate also competing with apotransferrin for ferric monocitrate. Kinetic differences between ferrotransferrin formation and cellular uptake from ferric citrate may explain the additional iron uptake from newly released mononuclear species before apotransferrin can chelate them altogether. The coordination sites on the iron (shown in bold) are typically occupied by water, but they are labile sites and can also bind oxygen and H_2O_2, rendering the species susceptible to redox chemistry (marked in bold cursive on the right). They are also the sites of condensation with other iron complexes.

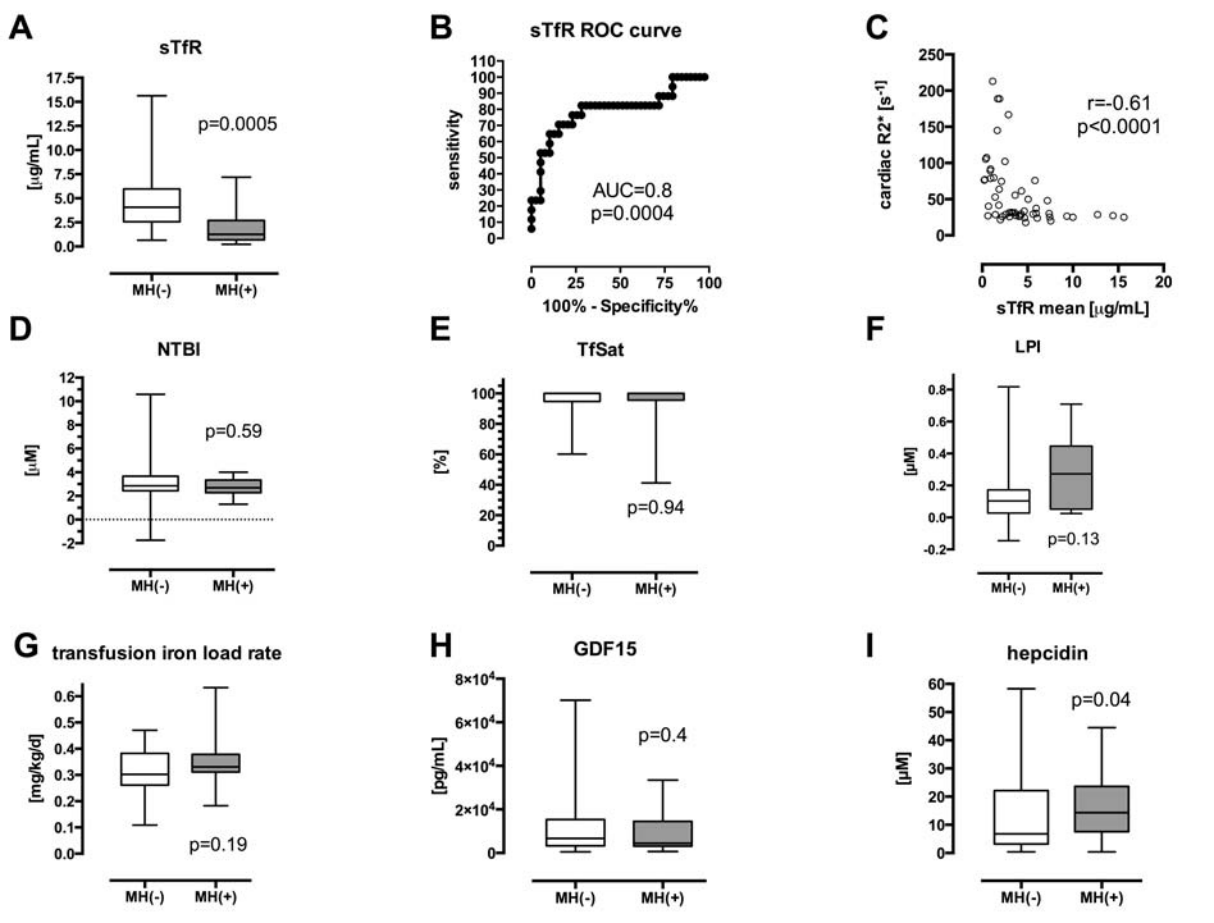
A
sTfR
[μg/mL]
p=0.0005
MH(-)
MH(+)
B
sTfR ROC curve
sensitivity
AUC=0.8
p=0.0004
100% - Specificity%
C
cardiac R2* [s-1]
r=-0.61
p<0.0001
sTfR mean [μg/mL]
D
NTBI
[μM]
p=0.59
MH(-)
MH(+)
E
TfSat
[%]
p=0.94
MH(-)
MH(+)
F
LPI
[μM]
p=0.13
MH(-)
MH(+)
G
transfusion iron load rate
[mg/kg/d]
p=0.19
MH(-)
MH(+)
H
GDF15
[pg/mL]
p=0.4
MH(-)
MH(+)
I
hepcidin
[μM]
p=0.04
MH(-)
MH(+)

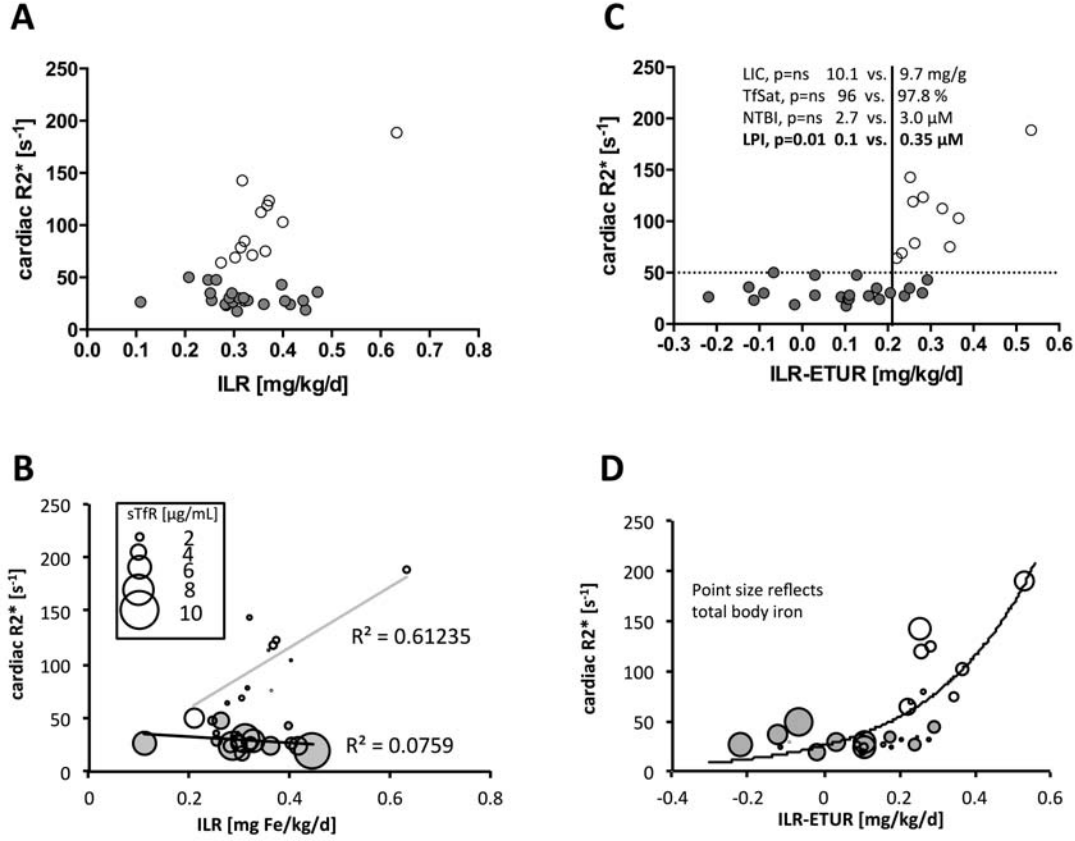
A
cardiac R2* [s-1]
ILR [mg/kg/d]
C
LIC, p=ns 10.1 vs. 9.7 mg/g
TfSat, p=ns 96 vs. 97.8 %
NTBI, p=ns 2.7 vs. 3.0 µM
LPI, p=0.01 0.1 vs. 0.35 µM
ILR-ETUR [mg/kg/d]
B
sTfR [µg/mL]
2
4
6
8
10
R² = 0.61235
R² = 0.0759
ILR [mg Fe/kg/d]
D
Point size reflects total body iron
ILR-ETUR [mg/kg/d]

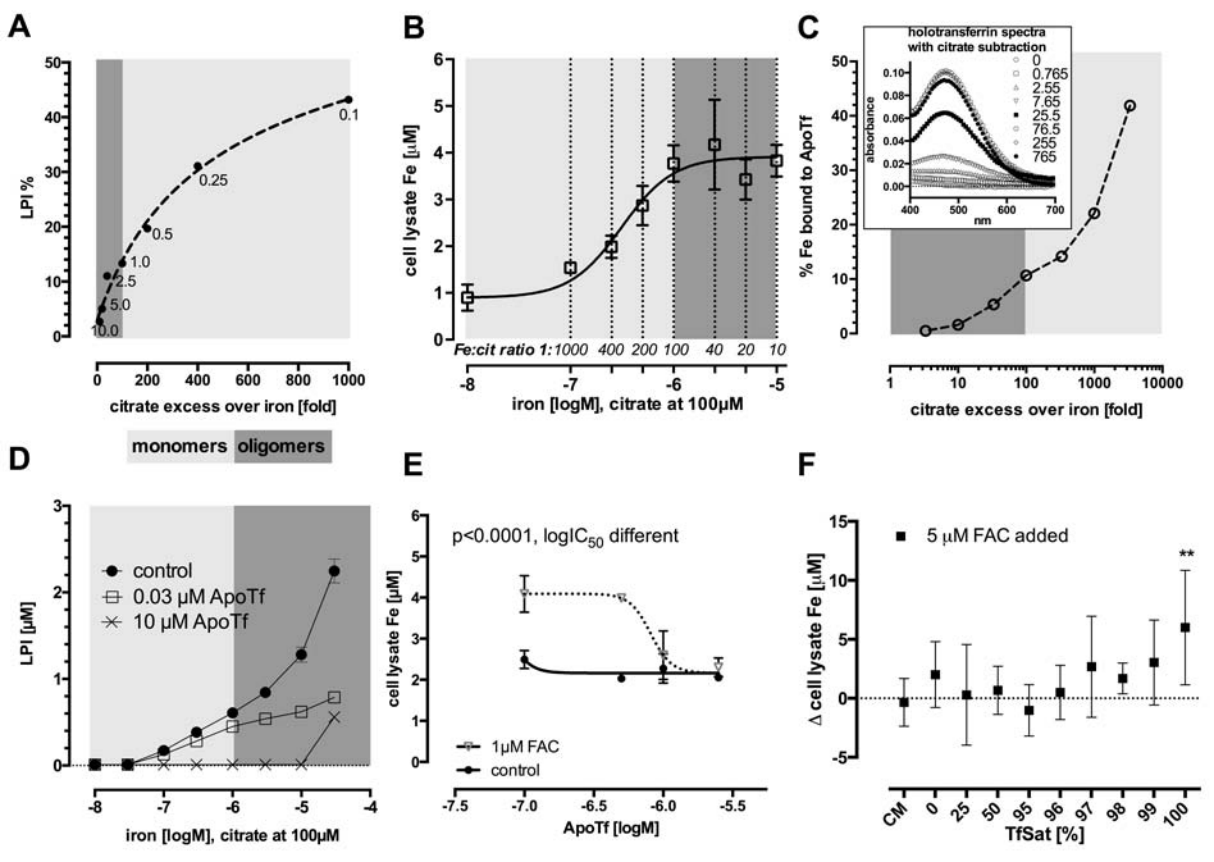
A
LPI %
0.1
0.25
0.5
1.0
2.5
5.0
10.0
citrate excess over iron [fold]
monomers
oligomers
B
cell lysate Fe [μM]
Fe:cit ratio 1: 1000 400 200 100 40 20 10
iron [logM], citrate at 100μM
C
holotransferrin spectra with citrate subtraction
absorbance
nm
0
0.765
2.55
7.65
25.5
76.5
255
765
% Fe bound to ApoTf
citrate excess over iron [fold]
D
LPI [μM]
control
0.03 μM ApoTf
10 μM ApoTf
iron [logM], citrate at 100μM
E
p<0.0001, logIC50 different
cell lysate Fe [μM]
1μM FAC
control
ApoTf [logM]
F
5 μM FAC added
**
Δ cell lysate Fe [μM]
CM
0
25
50
95
96
97
98
99
100
TfSat [%]

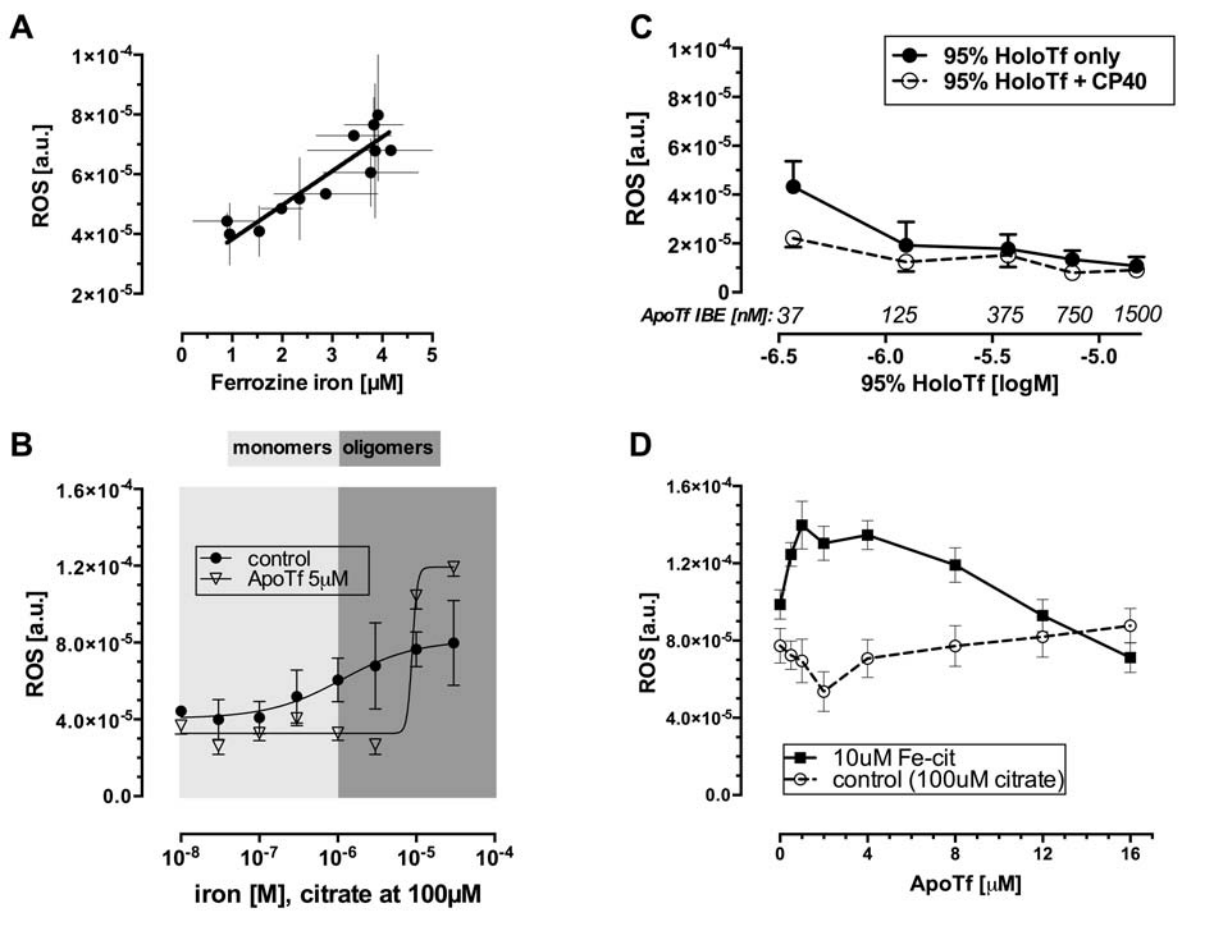
A
ROS [a.u.]
1×10-4
8×10-5
6×10-5
4×10-5
2×10-5
0 1 2 3 4 5
Ferrozine iron [μM]
B
monomers
oligomers
control
ApoTf 5μM
ROS [a.u.]
1.6×10-4
1.2×10-4
8.0×10-5
4.0×10-5
0.0
10-8 10-7 10-6 10-5 10-4
iron [M], citrate at 100μM
C
95% HoloTf only
95% HoloTf + CP40
ROS [a.u.]
1×10-4
8×10-5
6×10-5
4×10-5
2×10-5
0
ApoTf IBE [nM]: 37 125 375 750 1500
-6.5 -6.0 -5.5 -5.0
95% HoloTf [logM]
D
ROS [a.u.]
1.6×10-4
1.2×10-4
8.0×10-5
4.0×10-5
0.0
10uM Fe-cit
control (100uM citrate)
0 4 8 12 16
ApoTf [μM]

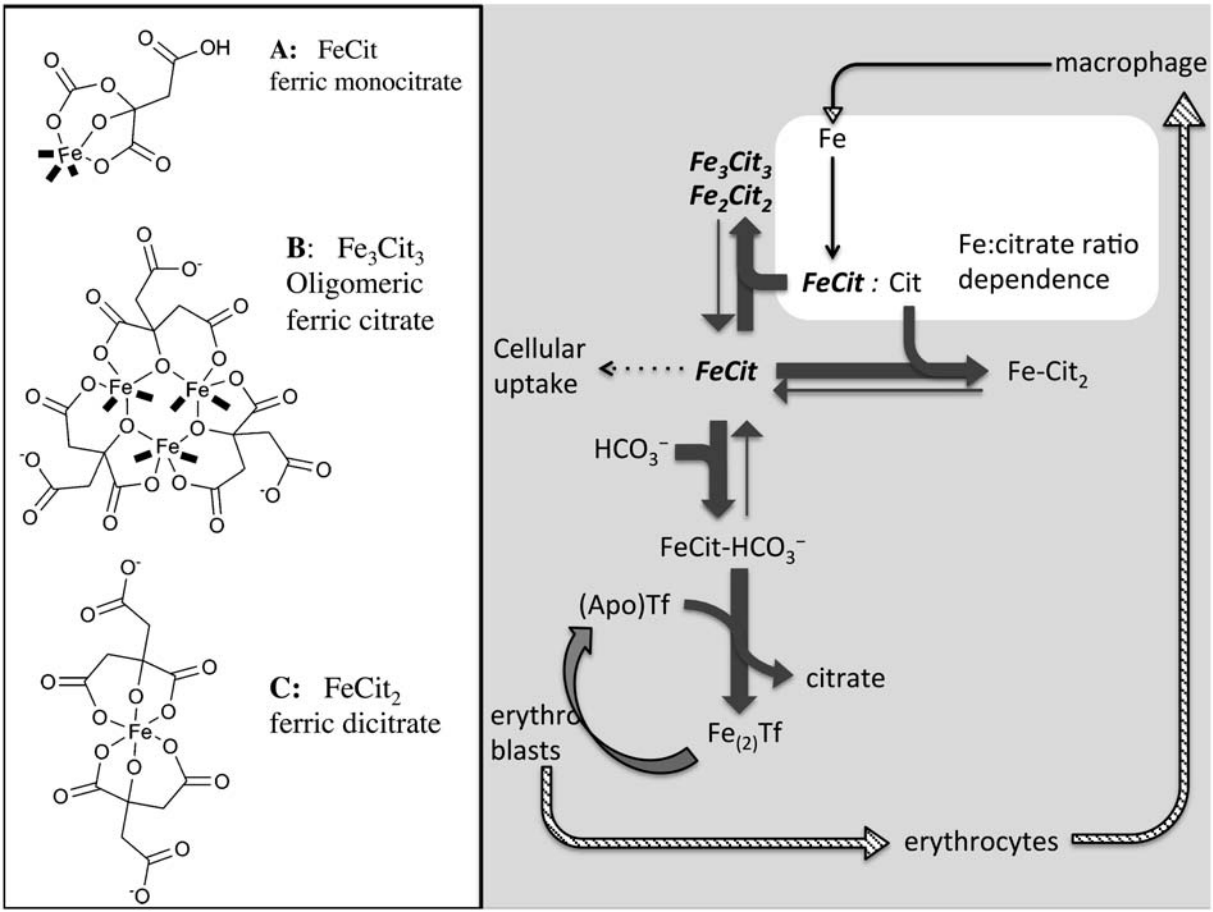
A: FeCit
ferric monocitrate
B: Fe_3Cit_3
Oligomeric
ferric citrate
C: $FeCit_2$
ferric dicitrate
macrophage
Fe
Fe_3Cit_3
Fe_2Cit_2
FeCit : Cit
Fe:citrate ratio
dependence
Cellular
uptake
FeCit
Fe-Cit_2
HCO_3^-
FeCit-HCO_3^-
(Apo)Tf
citrate
erythro
blasts
$Fe_{(2)}Tf$
erythrocytes

Supplement to

Residual erythropoiesis protects against myocardial hemosiderosis in transfusion-dependent thalassemia by lowering labile plasma iron via transient generation of apotransferrin.

Maciej W. Garbowski, Patricia Evans, Evangelia Vlachodimitropoulou, Robert Hider, John B. Porter

Methods

In order to relate cardiac iron to biomarkers in patient blood samples, cardiac MRI and blood biomarkers were measured at baseline and ~1.5 years later, over which time the **transfusion iron load rate (ILR)** in mg/kg/day was calculated from the number of blood units transfused, assuming 200mg iron per unit, patients' mean weight and number of days between MRI scans[1]. The mean follow-up was 502.7 days (SD 189.5), baseline mean cardiac R2* 61.14±5.8s^{-1}, follow-up 56.96±5.19s^{-1}(SE). During the follow-up, the change in the mean cardiac iron level was significant (paired t-test p=0.011), although clinically trivial, of 4.17 s^{-1}. The cohort of 73 patients with transfusion dependent thalassaemia on deferasirox was divided into those with MH (n=24, cardiac T2*<20ms, R2*>50s^{-1}) and those without MH (n=49, T2*>20ms, R2* <50s^{-1})[2].

Plasma biomarkers

A range of serum and plasma biomarkers was used in the study to test for a relationship with cardiac iron.

Non-transferrin-bound iron (NTBI) was assayed using the HPLC-based nitrilotriacetate (NTA) method[3,4]. Briefly, 20µL of 800mM NTA (at pH=7) was added to 180µl serum and allowed to stand for 30min at 22^{o}C. The solution was ultra-filtered using the 30kDa Whatman Vectaspin ultracentrifugation devices at 12320***g*** and the ultra-filtrate (20µL) was injected directly onto an HPLC column (ChromSpher-ODS, 5µM, 100x3mm, glass column fitted with an appropriate guard column) equilibrated with 5% acetonitrile and 3mM deferiprone in 5mM MOPS (pH=7.8). The NTA-iron complex then exchanges to form the deferiprone–iron complex detected at 460nm by a Waters 996 photo-diode array. Injecting standard concentrations of iron prepared in 80mM NTA generated a standard curve. The 800mM NTA solution used to treat the samples and prepare the standards is treated with 20µM iron to normalize the background iron that contaminates reagents. This means that the zero standard gives a positive signal since it contains the added background iron as an NTA–complex (2µM). When unsaturated transferrin is present in sera, this additional background iron can be donated to vacant transferrin sites resulting in a loss of the background signal and yielding a negative NTBI value.

Labile plasma iron (LPI) assay was performed in a cell-free system (on patient plasma in Figure 1, Figure 2 and Table 1 or on buffered solutions in Figure 3) using the 2,3-dihydrorhodamine (DHR) method[5] with modifications as previously published[6], which were limited to the generation of standards in plasma-like

medium containing 20mg/mL human serum albumin. The assay was recently used in an international round robin[7]. Briefly, in a 96-well plate, quadruplicates of 20µL of serum or buffered solution were added to 180µL of plasma-like medium, containing 20mg/mL human serum albumin and freshly added 50µM DHR with 40µM ascorbate only for the first set of duplicates and 40µM ascorbate with 50µM deferiprone for the second set of duplicates. Fluorescence intensity measurements were taken in each well (excitation 485nm, emission 538nm) for 40 minutes, with readings every 2 minutes. Slopes of DHR fluorescence intensity were taken between 15 and 40 minutes, and expressed as fluorescence intensity units per minute. The duplicate values of the slopes in the presence and absence of deferiprone (r_1 and r_2, respectively) were averaged and subtracted (r_2-r_1) for both the standards and the unknowns, with the LPI value of the unknowns interpolated from the standard curve. Standards were prepared from Fe-NTA (1:7) solutions spiked into plasma-like-medium.

Plasma hepcidin was assayed using mass-spectrometry[8], **transferrin saturation** was measured using the urea-gel method[9], **sTfR1** and **GDF-15** ELISAs were performed as before[10], according to manufacturers' specifications. Routine relevant haematological and biochemical biomarkers included automated **absolute reticulocyte count**, automated **nucleated red blood cell count** (NRBC), serum total **bilirubin**, **hemoglobin**, serum **ferritin**, and **total serum iron**.

Cell-line experiments on HL-1 cardiomyocytes

For cell-line experiments, murine HL-1 cardiomyocytes (ATCC number CRL-12197) were grown as previously published[11], on 80cm^2 flasks (SLS Ltd) or 48-well plates (Fisher Scientific, UK) coated with 0.5mL/100mL fibronectin (F-1141) in 0.02% gelatin (BD) in Claycomb medium supplemented with 300µM ascorbate, 100µM norepinephrine, 2mM L-glutamine, 100U/mL penicillin, 100µg/mL streptomycin and 10% fetal calf serum (serum batches for HL-1 cells as defined by SAFC). After confluence had been achieved (24-48h), monolayers were washed with Claycomb medium without FCS before subsequent 24h incubation with experimental media (culture media without FCS). Claycomb medium contains 1.76±0.03µM iron using ferrozine assay (see below) of which 0.8µM is transferrin iron, as per manufacturer's communication that typically 0.4µM holotransferrin is added during media production. PBS contains 2.57±0.19µM iron using ferrozine assay (see below), chelexed PBS contains 0.028±0.01µM iron.

Iron solutions for *in-vitro* work

In order for ferric iron to remain in solution at physiological pH=7.4, it needs to be liganded to protein, typically transferrin, or other ligands in order to prevent iron from being coordinated by water molecules – a process that eventually leads to precipitation as ferric hydroxide complexes. Citrate is the most relevant physiological ligand for ferric iron when transferrin is fully saturated[12]. As a model of NTBI, **ferric citrate buffered** in MOPS pH=7.4 was used following 24h incubation at room temperature after its preparation to allow for species stabilization[13,14]. During its preparation atomic absorption 18.036mM ferric chloride standard was mixed with 80mM sodium citrate at specified ratios and left for 30 minutes to equilibrate. Careful drop-wise addition of buffered MOPS pH=7.4, under

constant vortex-mixing, slowly (1-2min for each solution) increased the pH and then the solution was left to allow for species stabilisation. In the buffered solutions containing iron-to-citrate ratios of 1:3333, 1:1000, 1:333, 1:100, 1:33, 1:10, and 1:3.3, the ferric citrate species range from *predominantly* ferric dicitrate ($FeCit_2$, up to 1:100) through dimers (Fe_2Cit_2) and trimers (Fe_3Cit_3) and their stacks[13,14]. Because there exists a relationship between iron-to-citrate ratios in the solution and the predominant species present, i.e. that ratio determines the ferric citrate speciation, we also refer to the species by stating the relevant *causal* iron-to-citrate ratio, e.g. 1:100 species typically indicates a monomeric species such as the ferric dicitrate species $FeCit_2$, since under pH=7.4 it is the *predominant* form of ferric citrate present in 1:100 iron-to-citrate ratio solutions. We prepared ferric citrate solutions with constant citrate (at physiological concentration of 100μM). After species stabilization (i.e. at 24h from preparation), ferric citrate solutions were incubated in Claycomb medium with *confluent* HL-1 cardiomyocytes for 24 hours. When **ferric ammonium citrate (FAC)** was used, it was added as freshly prepared (from solids) to the experimental media. Freshly dissolved ferric ammonium citrate is a 1:2 Fe:citrate ratio ferric citrate (i.e. constant ratio ferric citrate) with inert ammonium cations in solution[15]. For the sake of simplicity we have not used albumin alongside ferric citrate to model NTBI.

Ferrotransferrin preparation

In order to produce diferric transferrin, apotransferrin was saturated using ferric nitrilotriacetate (Fe-NTA) in excess of transferrin binding (or to 95%) with subsequent 24h dialysis against 2L of PBS using 10,000 MWCO Slide-A-Lyzer Dialysis Cassette (Thermo Scientific) to remove excess iron and NTA. Transferrin saturation solutions were prepared by mixing thus obtained diferric transferrin with calculated amounts of MOPS-buffered apotransferrin in 25mM bicarbonate to obtain the nominal % saturation of transferrin. In this model of transferrin saturation, the monoferric transferrin species are not present, which may be considered a limitation of this model, however in our experiments we wished to address the nascence of apotransferrin which, unlike the monoferric species, is the consequence of uptake and recirculation of diferric (and monoferric) transferrin by the erythron[16].

The **viability** of HL-1 cardiomyocytes, in the presence of 0-30μM buffered ferric citrate ± 5μM apotransferrin, was 96.6±0.7%, as assessed by the electric current exclusion method on CASY Model TT Cell Counter and Analyzer (Roche).

Cellular iron assays

Total cellular iron was assayed by **ferrozine** using previously published methods[17]. Briefly, following incubation of cell monolayers in experimental media, cells were washed 3-4 times with PBS (including one wash with DFO- or CP40-containing PBS to remove membrane associated iron). Washed monolayers were then lysed with 200μL of 200mM NaOH and left overnight on a plate shaker. A 100μL aliquot of the lysate was added to 100μL of 100μM HCl (standard solution matrix) and treated with 100μL of a freshly prepared iron-extracting solution (1:1 vol/vol 5% $KMnO_4$/1.4M HCl) for 2h at 60°C under fume hood extraction. This was followed by the addition of 30μL of a freshly prepared iron-detecting solution, containing

6.5mM ferrozine, 6.5mM neocuproine, and 1M ascorbic acid in 2.5M ammonium acetate, and the mixture was incubated for 30 minutes at room temperature on an orbital plate shaker. The absorbance of the ferrozine-iron complex was measured at 562nm using a plate-reader. Results were interpolated from a standard curve obtained using atomic absorption ferric chloride standards and 100µL of 200mM NaOH (lysate matrix) and reported as cell lysate iron concentration (µM).

Reactive Oxygen Species assay

The intracellular reactive oxygen species (ROS) assay was performed using 2,7-dichlorofluorescein diacetate (H_2DCF-DA), which is de-esterified intracellularly by live cells to 2,7-dichlorofluorescein (DCF). 9µM H_2DCF-DA in DMSO/PBS was added to confluent HL-1 monolayers after PBS rinse and incubated for 30 min in 48-well plates at 37°C and 5% CO_2. Following three PBS rinses, 500µL PBS aliquot was added with 100µM CP40 or 5µM apotransferrin (final concentration). CP40 chelator was used as a control for extra-cellular chelation[18]. Immediately afterwards, ferric citrate, buffered in MOPS pH=7.4, was added to a final concentration of 0-30µM. Fluorescence was monitored for 60 minutes (excitation 493nm, emission 523nm). Slopes, shown as mean±SD, were calculated from fluorescence-versus-time data to represent the cytosolic ROS formation over 1h using linear regression.

The extracellular chelator CP40 was a kind gift from Professor Robert Hider, KCL. All chemicals were from Sigma-Aldrich apart from 0.05% trypsin-EDTA, L-glutamine, streptomycin and penicillin (Life Technologies), soybean trypsin inhibitor (Invitrogen), atomic absorption ferric chloride standard (Aldrich), ammonium acetate (Fisher) or if otherwise stated.

Supplemental Figures:

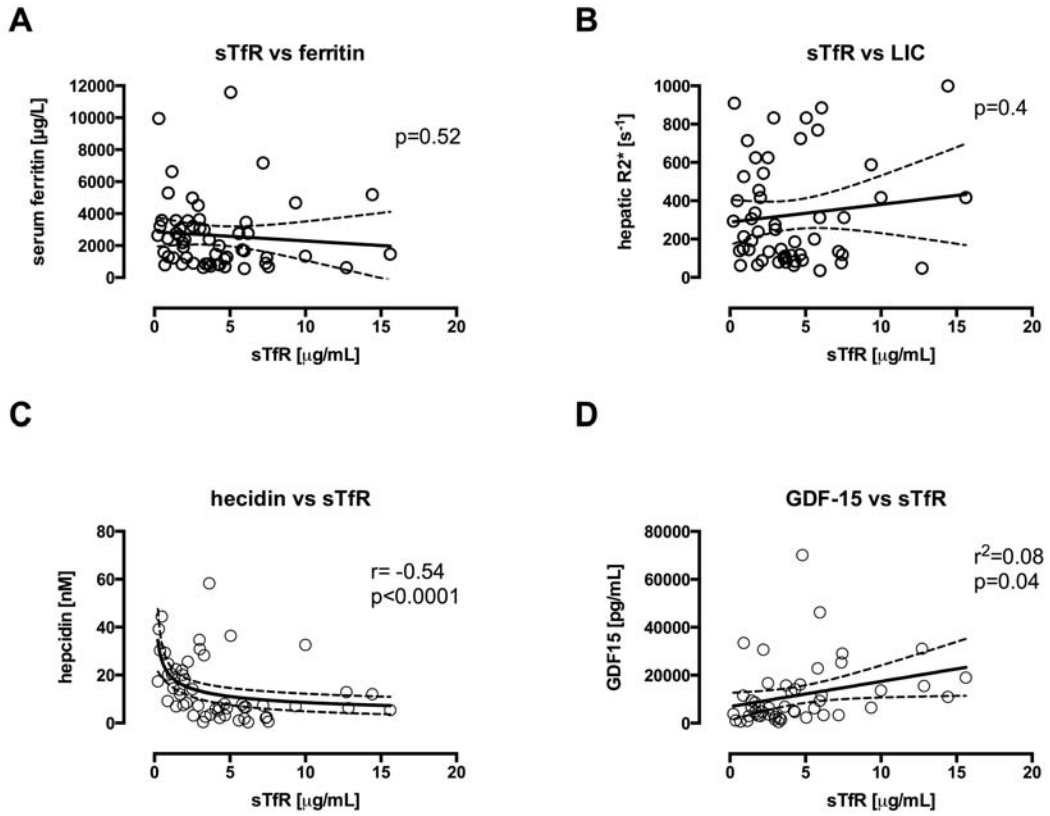

Supplement Figure 1. The correlations and regressions of soluble transferrin receptor-1 (sTfR1) with markers of iron overload, hepcidin and GDF-15.
(A) Relationship of serum ferritin and sTfR1, linear regression slope p=0.52. (B) Relationship of hepatic R2* with sTfR1, linear regression slope p=0.4. (C) Relationship of plasma hepcidin and sTfR1, Spearman correlation coefficient r= -0.54, p<0.0001; power series regression $y=20.06[\pm 2.09]x^{-0.37[\pm 0.09]}$. (D) Relationship of GDF-15 and sTfR1, linear regression slope p=0.04.

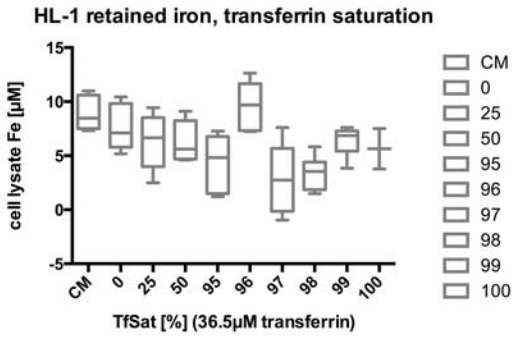

Supplement Figure 2. Dose response of iron retention in HL-1 cells to transferrin saturation.
Confluent HL-1 cardiomyocytes were incubated for 24h with Claycomb medium, containing 36.5µM transferrin concentration, with transferrin saturation obtained by mixing diferric transferrin to apotransferrin at specified ratios, mean±SD, n=6; see methods.

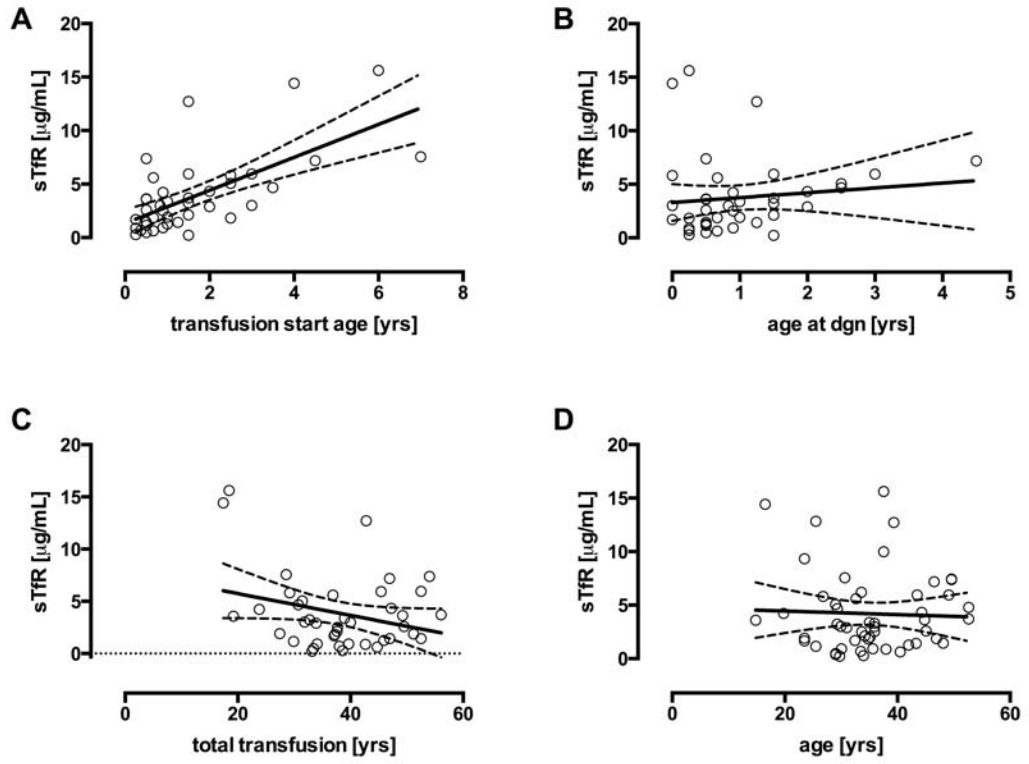

Supplemental Figure 3. The relationship of patient history factors to sTfR1 in TDT. (A) Regression of sTfR on the age when chronic transfusion was started, slope p<0.0001. (B) Regression of sTfR on age at diagnosis, slope p=0.47. (C) Regression of sTfR on the total duration of transfusion dependence, slope p=0.07. (D) Regression of sTfR on patient's age, slope p=0.77.

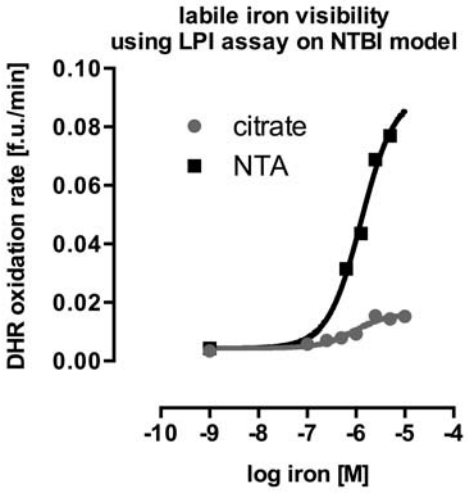

Supplemental Figure 4. Labile plasma iron for ferric nitrilotriacetate and ferric citrate species is shown.
Labile plasma iron (LPI) assay performed using 0-10µM ferric nitrilotriacetate and 0-10µM ferric citrate at constant citrate (100µM), mean±SD, n=2; see methods.

References

1. Cohen AR, Glimm E, Porter JB. Effect of transfusional iron intake on response to chelation therapy in β-thalassemia major. *Blood*. 2008;111(2):583–587.
2. Anderson LJ, Holden S, Davis B, et al. Cardiovascular T2-star (T2*) magnetic resonance for the early diagnosis of myocardial iron overload. *Eur. Heart J.* 2001;22(23):2171–2179.
3. Singh S, Hider RC, Porter JB. A direct method for quantification of non-transferrin-bound iron. *Anal. Biochem.* 1990;186(2):320–323.
4. Porter JB, Abeysinghe RD, Marshall L, Hider RC, Singh S. Kinetics of removal and reappearance of non-transferrin-bound plasma iron with deferoxamine therapy. *Blood*. 1996;88(2):705–13.
5. Esposito BP, Breuer W, Sirankapracha P, et al. Labile plasma iron in iron overload: Redox activity and susceptibility to chelation. *Blood*. 2003;102(7):2670–2677.
6. Lal A, Porter J, Sweeters N, et al. Combined chelation therapy with deferasirox and deferoxamine in thalassemia. *Blood Cells, Mol. Dis.* 2013;50(2):99–104.
7. de Swart L, Hendriks JCM, van der Vorm LN, et al. Second international round robin for the quantification of serum non-transferrin-bound iron and labile plasma iron in patients with iron-overload disorders. *Haematologica*. 2015;101(1):38–45.
8. Bansal SS, Halket JM, Fusova J, et al. Quantification of hepcidin using matrix-assisted laser desorption/ ionization time-of-flight mass spectrometry. *Rapid Commun. Mass Spectrom.* 2009;23(11):1531–1542.
9. Evans RW, Williams J. The electrophoresis of transferrins in urea/polyacrylamide gels. *Biochem. J.* 1980;189(3):541–546.
10. Porter JB, Walter PB, Neumayr LD, et al. Mechanisms of plasma non-transferrin bound iron generation: Insights from comparing transfused diamond blackfan anaemia with sickle cell and thalassaemia patients. *Br. J. Haematol.* 2014;167(5):692–696.
11. Claycomb WC, Lanson N a, Stallworth BS, et al. HL-1 cells: a cardiac muscle cell line that contracts and retains phenotypic characteristics of the adult cardiomyocyte. *Proc. Natl. Acad. Sci. U. S. A.* 1998;95(6):2979–2984.
12. Grootveld M, Bell JD, Halliwell B, et al. Non-transferrin-bound iron in plasma or serum from patients with idiopathic hemochromatosis. Characterization by high performance liquid chromatography and nuclear magnetic resonance spectroscopy. *J. Biol. Chem.* 1989;264(8):4417–4422.
13. Evans RW, Rafique R, Zarea A, et al. Nature of non-transferrin-bound iron: Studies on iron citrate complexes and thalassemic sera. *J. Biol. Inorg. Chem.* 2008;13(1):57–74.
14. Silva AMN, Kong X, Parkin MC, Cammack R, Hider RC. Iron(III) citrate

speciation in aqueous solution. *Dalton Trans.* 2009;(40):8616–8625.

15. Matzapetakis M, Raptopoulou CP, Tsohos A, et al. Synthesis, Spectroscopic and Structural Characterization of the First Mononuclear, Water Soluble Iron−Citrate Complex, (NH4)5Fe(C6H4O7)2·2H2O. *J. Am. Chem. Soc.* 1998;120(10):13266–13267.

16. Huebers HA, Finch CA. The physiology of transferrin and transferrin receptors. *Physiol. Rev.* 1987;67(2):520–582.

17. Riemer J, Hoepken HH, Czerwinska H, Robinson SR, Dringen R. Colorimetric ferrozine-based assay for the quantitation of iron in cultured cells. *Anal. Biochem.* 2004;331(2):370–375.

18. Vlachodimitropoulou Koumoutsea E, Garbowski M, Porter J. Synergistic intracellular iron chelation combinations: Mechanisms and conditions for optimizing iron mobilization. *Br. J. Haematol.* 2015;170(6):874–883.